Available online at www.sciencedirect.com
SCIENCE DIRECT
Journal of Catalysis 240 (2006) 126–136
JOURNAL OF CATALYSIS
www.elsevier.com/locate/jcat

Continuous catalytic oxidation of solid alcohols in supercritical CO_2: A parametric and spectroscopic study of the transformation of cinnamyl alcohol over Pd/Al_2O_3

Matteo Caravati, Daniel M. Meier, Jan-Dierk Grunwaldt *, Alfons Baiker

Institute for Chemical and Bioengineering, Department of Chemistry and Applied Biosciences, ETH Zurich, Hönggerberg, HCI, 8093 Zurich, Switzerland

Received 9 January 2006; revised 14 March 2006; accepted 17 March 2006

Available online 24 April 2006

Abstract

Cinnamyl alcohol was oxidized to cinnamaldehyde in a continuous fixed-bed reactor with molecular oxygen over an alumina-supported palladium catalyst in supercritical carbon dioxide modified with toluene. A strong dependence of the reaction performance on pressure and oxygen concentration in the feed was found. Optimization of the reaction conditions resulted in a higher catalytic activity than in the liquid phase. At 120 bar, 80 °C, and double stoichiometric oxygen concentration, a turnover frequency of 400 h^{-1} at a selectivity of 60% to cinnamaldehyde was achieved. Spectroscopic investigations and the knowledge of the selectivity pattern turned out to be crucial for a deeper understanding of the reaction allowing a rational optimization. Under almost all experimental conditions (even at high oxygen concentration) hydrogenated byproducts, stemming from internal hydrogen transfer reactions, were detected in the effluent. This indicated that alcohol dehydrogenation was the first reaction step; this finding was further confirmed by spectroscopic investigations. In situ XANES and EXAFS revealed that in the entire experimental range investigated, the palladium constituent was mainly in a reduced state, and its surface could be oxidized only in the absence of cinnamyl alcohol in the feed. Bulk-phase behavior studies and investigations at the catalyst–fluid interface, performed by visual inspection and combined transmission and ATR-IR spectroscopy, demonstrated that the reaction performed best in the biphasic region. Moreover, cinnamaldehyde and carbon dioxide, but hardly any toluene and cinnamyl alcohol, were detected inside the porous catalyst, indicating a significantly different product composition inside the porous catalyst compared with the bulk phase.

Keywords: Aerobic oxidation; Cinnamyl alcohol; Supercritical CO_2; Phase behavior; In situ ATR-IR; In situ EXAFS; Operando spectroscopy

1. Introduction

Supercritical carbon dioxide is well suited as a solvent for oxidation reactions because of its natural abundance, nontoxicity, and inertness, which result in safer operation. Moreover, it is fully miscible with molecular oxygen (air) and exhibits high heat capacity [1–10]. Compared with most conventional solvents, supercritical CO_2 also results in improved internal and external mass transport, often leading to an enhanced global reaction rate. This is especially valid under single-phase conditions [1,2,9,11,12].

Among heterogeneously catalyzed oxidation reactions, the selective oxidation of alcohols to the corresponding aldehyde or ketone is important in fine chemistry [13–16]. These reactions are typically performed under mild conditions over noble metal-supported catalysts, using water as a solvent and molecular oxygen or air as the sole oxidant. For weakly polar alcohols, poorly soluble in water, the use of supercritical CO_2 has proven beneficial, precluding the need for detergents or organic solvents [17,18] and thus leading to a safer and more environmentally friendly process. In several cases, higher rates and selectivity than the ones obtained in conventional solvents, as well as improved catalyst lifetime, were reported [17–21]. The reactions were performed either in a batch reactor or in a continuous fixed-bed reactor in a wide temperature and pressure range. Optimal reaction conditions often depend signifi-

* Corresponding author.
E-mail address: grunwaldt@chem.ethz.ch (J.-D. Grunwaldt).

0021-9517/$ – see front matter
doi:10.1016/j.jcat.2006.03.009

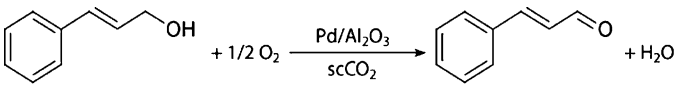

Scheme 1. Reaction scheme of cinnamyl alcohol oxidation to cinnamaldehyde with molecular oxygen in supercritical CO_2 over an alumina-supported palladium catalyst.

cantly on the catalyst, the substrate, and also the reactor type. Deeper spectroscopic insight into such oxidation reactions has been gained only recently [17,20,22,23]. Significantly different features compared to liquid-phase oxidation have been demonstrated. However, up to now, these kind of studies have been limited.

In the fine chemicals industry, many of the commercially interesting alcohols are solid. Only a few studies on the selective oxidation of solid alcohols using supercritical CO_2 as a solvent have been reported [18,21], and in those studies discontinuous reactors (batch reactors) were applied. Here we propose a simple approach to continuously oxidize solid alcohols with molecular oxygen in supercritical CO_2. The method involves dissolving the solid alcohol in a small amount of a liquid organic solvent and continuously feeding it as a reaction mixture via a liquid pump. One advantage of this method is the flexible setup that allows continuous processing of both liquid and solid alcohols without losing the technical and environmental benefits of supercritical CO_2 (i.e., nonflammability, process intensification, improved mass and heat transfer). Moreover, the alcohol can be easily dosed, and using a co-solvent can prevent possible blocking of tubing and valves.

The present work focused on the oxidation of the solid and technically relevant cinnamyl alcohol (Scheme 1). The influence of the main process variables (pressure, temperature, co-solvent amount, oxygen concentration) on the reaction rate and on the product/byproduct distribution was studied. In previous studies, we showed that a profound knowledge of the phase behavior, the solid–fluid interface, and the catalyst structure is vitally important for reactions in supercritical fluids [9,12,20, 23]. Moreover, even in liquid phase, controversy exists regarding the nature of the active site and the reaction mechanism [13,14,16,24,25]. Both oxidized palladium and metallic Pd sites have been speculated to be the active species in the reaction.

Hence, complementary to the catalytic activity measurements, in situ spectroscopic studies are required for a rational process optimization. In the present study, we applied both in situ infrared spectroscopy (in transmission and attenuated total reflection [ATR] mode) combined with video monitoring and in situ X-ray absorption spectroscopy (XAS). Although the IR/visual inspection studies could provide insight into the phase behavior of the reaction mixture and the phenomena occurring at the catalyst–fluid interface during the reaction, XAS was used to gain insight into the catalyst structure under reaction conditions. Additional insight into the reaction mechanism was gained by the selectivity pattern observed during cinnamyl alcohol oxidation, because the substrate can undergo different side reactions (Scheme 2) [24,26].

2. Experimental

2.1. Catalytic measurements

The reactions were performed isothermally in a fixed-bed stainless steel tubular reactor with an inner diameter of 13 mm and a volume of 38 mL. The temperature of the catalyst bed was monitored by an axially movable thermocouple placed in the center of the reactor. A commercial shell-impregnated catalyst consisting of 0.5 wt% Pd/Al_2O_3 (Engelhard 4586) was crushed and used as a sieved fraction (ca. 0.5–1.4 mm). Pure alumina (Engelhard 43299) of the same sieved fraction was used to dilute the catalyst bed, to avoid possible hot spot formation by the exothermic reaction. Then 2.5 g of catalyst and 1.5 g of alumina were loaded, corresponding to a bed length of ca. 4 cm. Glass beads were placed above the catalyst to ensure optimal distribution of the reactants at the entrance of the catalytic bed. The catalyst was prereduced with H_2 before starting the measurements, to improve its stability and guarantee its complete initial reduction. Cinnamyl alcohol (Fluka, 96330, purity $\geqslant$97.0%) and toluene (Fluka, 89681, purity >99.7) were used as received. Typically, 10 g of cinnamyl alcohol (melt-

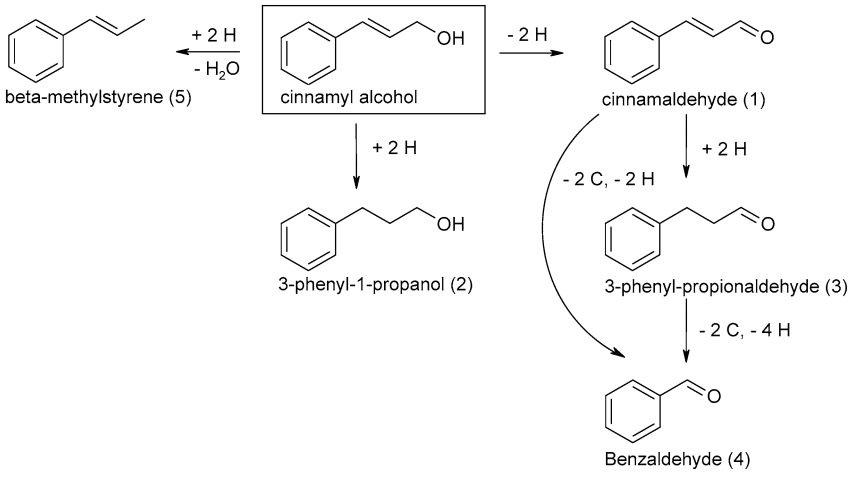

Scheme 2. Reaction network observed during the oxidation of cinnamyl alcohol with molecular oxygen in supercritical CO_2 over a supported palladium catalyst. Byproducts detected only in traces are not included.

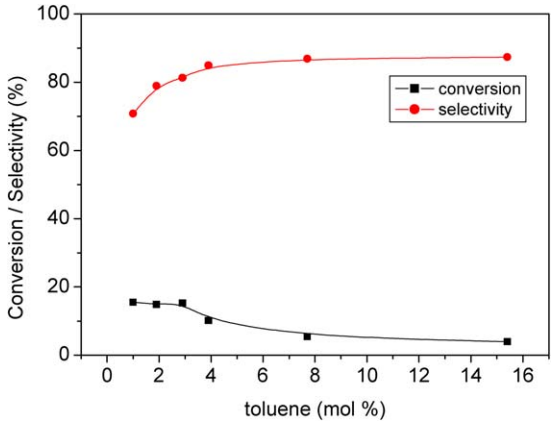

Fig. 1. Dependence of cinnamyl alcohol conversion and selectivity to cinnamaldehyde on the concentration of toluene in the feed. The data were obtained over a stabilized (equilibrated) catalyst; conditions: 150 bar, 80 °C, 3.55×10^{-4} mol/min cinnamyl alcohol, 3.55×10^{-4} mol/min O_2, 0.233 mol/min CO_2, 2.5 g of 0.5 wt% Pd/Al_2O_3.

ing point 30–33 °C, technical purity) were dissolved in 100 mL of toluene (corresponding to a molar concentration of toluene of 1.9%; Fig. 1), with the exception of experiments in which the amount of toluene was varied to check its influence on the reaction performance. The cinnamyl alcohol/toluene mixture was fed to the reactor by a Gilson 305 HPLC pump with a volumetric liquid flow of 0.482 mL/min, resulting in an alcohol molar flow rate of 3.55×10^{-4} mol/min. Oxygen (Pangas, purity $\geqslant$99.999%) was supplied through a six-port switching valve (Rheodyne, model 7000) dosing 0.05- or 1-mL pulses at high pressure and constant frequency. The constant pressure was maintained by a pressure regulator with CO_2, and the total gas flow was controlled at the vent. Product identification was performed by GC/MS (HP-5973), and quantitative results were obtained via GC analysis (HP-6890, FFAP column). Details on the experimental setup can be found elsewhere [17].

2.2. FTIR and phase behavior measurements

Infrared spectroscopic investigations were carried out in a custom-made stainless steel high-pressure view cell (SITEC AG) that can withstand pressures up to 200 bar and temperatures up to 200 °C. A sapphire window covering the entire diameter allows visual observation and digital imaging of the bulk-phase behavior. The cell is also equipped with IR transmission windows (ZnSe, Komlass, internal diameter 8 mm, length 19.2 mm) that allow transmission IR measurements in the upper part of the reactor (path length of 0.4 mm). An internal reflection element (IRE, Komlass, made of ZnSe, trapezoidal shape, angle of incidence 60°, length 27 mm, height 2 mm, depth 10 mm) mounted at the bottom of the hollow cylinder allows ATR-IR measurements. A motor-driven carriage moves a set of mirrors that directs the light beam either to the IRE or to the transmission windows, thus allowing quasi-simultaneous transmission IR and ATR-IR measurements. Fourier transform infrared (FTIR) spectra were recorded with a Bruker Optics IFS-66/s spectrometer equipped with a liquid nitrogen-cooled MCT detector, typically accumulating 200 scans at a resolution of 4 cm^{-1}. To perform the experiments, first the alcohol with toluene was loaded, then CO_2 was fed into the cell at 40 °C, and finally the desired pressure was adjusted by heating to 80 °C and changing the volume. The pressure was increased from 120 to 160 bar and then back again to 120 bar while recording both transmission IR and ATR-IR spectra after each pressure change of 5 bar. Detailed descriptions of a similar experimental setup and of the experimental procedure are available elsewhere [23,27]. To coat the IRE with a thin catalytic layer, 5 mg of 5 wt% Pd/Al_2O_3 (Johnson–Matthey, 324) was suspended in 0.5 mL of water. The suspension was placed onto the crystal, which was then dried overnight in air at room temperature.

2.3. XAS measurements

In situ XAS experiments were performed in a specially constructed flow cell (details in Ref. [22]) at the Hamburger Synchrotronlabor (HASYLAB at DESY, Germany) at beamline X1 using a Si(311) double-crystal monochromator. The crystals were slightly detuned to minimize higher harmonics, and three ionization chambers filled with Ar were used to record the intensity of the incident and transmitted X-ray beam. A Pd reference foil was used for energy calibration. EXAFS spectra were recorded around the Pd K-edge in the step-scanning mode between 24000 and 25600 eV. The raw data were energy-calibrated, smoothed, background-corrected, and normalized using WINXAS 3.0 software [28]. The k^3-weighted EXAFS data were Fourier-transformed in the interval $k = 2.7$–13 $Å^{-1}$. The in situ flow cell provides optimal conditions for the simultaneous monitoring of both catalyst structure and catalytic activity [22]. The catalyst and the substrate/solvents used during the operando XAS measurements were the same as those used during the catalytic experiments in the conventional reactor. Cinnamyl alcohol conversion and selectivity to cinnamaldehyde were determined by GC analysis (HP-6890, FFAP column).

3. Results

3.1. Catalyst and co-solvent screening

The selective oxidation of cinnamyl alcohol to cinnamaldehyde (Scheme 1) was performed in a continuous-flow reactor using supercritical CO_2 as a solvent and molecular oxygen as an oxidant. The solid cinnamyl alcohol was dissolved in a fixed amount of organic co-solvent and then fed to the reactor as a liquid solution in a continuous way. As a first preliminary step, screening to identify the best catalyst and a suitable co-solvent was performed, using the same activation procedure each time. The catalysts were tested over one day; the results are reported in Table 1. Palladium supported on alumina turned out to be the only active catalyst. In addition, performing the reaction with cinnamyl alcohol dissolved in toluene provided better performance than that dissolved in acetone and THF, both in terms of conversion and selectivity to aldehyde. Therefore, all further investigations were performed over a 0.5 wt% Pd/Al_2O_3 using toluene as a co-solvent.

Table 1
Conversion of cinnamyl alcohol and selectivity to cinnamaldehyde measured during oxidation with molecular oxygen in supercritical carbon dioxide modified with different co-solvents and over different catalysts; in all cases the catalyst was prereduced in the same manner at 100 °C and the catalytic data were recorded during the first day[a]

Catalyst	Co-solvent	Conversion (%)	Selectivity (%)
0.5 wt% Ru/Al_2O_3 (Engelhard 4871)	Toluene	–[b]	–[b]
0.5 wt% Pt/Al_2O_3 (Engelhard 4751)	Toluene	–[b]	–[b]
0.5 wt% Pd/Al_2O_3 (Engelhard 4586)	Toluene	60	71.5
0.5 wt% Pd/Al_2O_3 (Engelhard 4586)	Acetone	44.3	62.8
0.5 wt% Pd/Al_2O_3 (Engelhard 4586)	THF	33.3	64.3

[a] Conditions: 150 bar, 80 °C, 0.15 mol% cinnamyl alcohol, 0.15 mol% O_2, 1.9 mol% co-solvent in CO_2.
[b] Below detection limit of GC.

3.2. Reaction performance in toluene-modified dense CO_2

In the next step, the effect of toluene concentration on the reaction performance was investigated; the results are reported in Fig. 1. A constant reaction rate was found on increasing the amount of toluene from 1 to 2.9 mol%, with an alcohol conversion of ca. 15% and enhanced selectivity with an increasing amount of co-solvent. Increased amounts of toluene resulted in lower activity (conversion ca. 5% at 15.4 mol% toluene), even though the selectivity to the aldehyde kept increasing. On the basis of these results, it was decided to perform the parametric study presented in this work at a toluene concentration of 1.9 mol%, which seems to represent a good compromise between the amount of toluene added, catalytic activity, and selectivity to aldehyde. Note that at a lower toluene concentration of 1 mol%, unstable setup conditions were observed, with the CO_2 flow rate oscillating slightly around the desired value. This was probably due to the formation of solid substances in the expansion valves, which could be avoided by applying a higher amount of co-solvent. Co-solvents [29–31] and expanded liquids [32,33] have also been used in other studies to overcome solubility limitations [34,35] and in general to tune the solvent properties of SCFs without spoiling their advantageous properties [36,37]. In some cases, higher reaction rates than in neat CO_2 were reported, indicating that the co-solvent may play a crucial role in phase behavior, mass transfer properties, and adsorption/desorption phenomena [29–31,38]. A similar role of the co-solvent cannot be excluded in the present case, and thus toluene probably should not be considered only as a means of dissolving the solid alcohol. In principle, other solutions to process the solid cinnamyl alcohol alone, without a co-solvent, could be used; for example, injection of melted alcohol or the saturation method. However, these solutions would have required a more complex experimental setup for dosing the alcohol and for preventing possible solid deposit formation.

3.3. Catalyst deactivation

In contrast to previous studies on the selective oxidation of benzyl alcohol in $scCO_2$, in the case of cinnamyl alcohol, the palladium catalyst demonstrated significant deactivation during the first working days, with the alcohol conversion in a standard experiment dropping from 60% on the first day to 14.9% on the fifth day. In contrast, the selectivity to cinnamaldehyde increased from 72 to 79%. An increase in selectivity with decreasing conversion has been observed in other sets of experiments as well, and it can be considered a general feature of this reaction under the reaction conditions typically applied in the present study. Interestingly, after about 5 working days, no further deactivation was observed, and the catalyst demonstrating steady-state behavior was used for the parametric studies.

3.4. Reaction network

During the catalytic tests, different byproducts were detected in the effluent and identified by GC/MS. Byproducts originating from hydrogenation, hydrogenolysis, decarbonylation, and carbon–carbon double-bond cleavage were observed, but only some of them were present in appreciable amounts and thus taken into account in the reaction network shown in Scheme 2. Note, in the following, we refer to the number appearing in brackets after the product name for describing the compounds formed.

3.5. Systematic catalytic investigations

On the basis of the previous results, a parametric study was performed over a stabilized 0.5 wt% Pd/Al_2O_3 catalyst using toluene as a co-solvent. The influence of the total pressure on conversion and selectivity to cinnamaldehyde is reported in Fig. 2a. In the low-pressure region, a slight increase in conversion with increasing pressure was observed. A maximum was reached at 120 bar, with the turnover frequency (TOF) increasing up to 400 h^{-1}. At 130–140 bar, a sharp drop in conversion occurred, with a TOF of 90 h^{-1} at 150 bar. This behavior is in contrast to previous observations for benzyl alcohol [23], and we discuss it later in the light of phase behavior and X-ray absorption spectroscopy results. In contrast, the selectivity to cinnamaldehyde constantly increased with pressure, showing a more marked jump between 130 and 140 bar, corresponding to the drop in reaction rate. At 120 bar, where the maximum reaction rate was observed, the selectivity to cinnamaldehyde was 58.4%. Fig. 2b shows the product/byproduct distribution, revealing that the main product cinnamaldehyde is always present in the highest concentration. In the low-pressure region (corresponding to the higher catalytic activity) the two hydrogenated byproducts, 3-phenyl-1-propanol (2) and beta-methylstyrene (5), are present in comparable amounts to cinnamaldehyde (1).

Another important variable that has a significant effect on reaction performance is the oxygen concentration in the feed. Two sets of experiments at 120 and 150 bar were performed with varying oxygen concentrations up to 10 mol% (Figs. 3 and 4). In a test performed without oxygen feed, similar catalytic activity was measured at 120 bar (cinnamyl alcohol conversion of 12.4%) and 150 bar (conversion of 13%), with differing selectivities to cinnamaldehyde (57.6% at 120 bar vs. 79% at 150 bar). The dehydrogenation via internal hydrogen

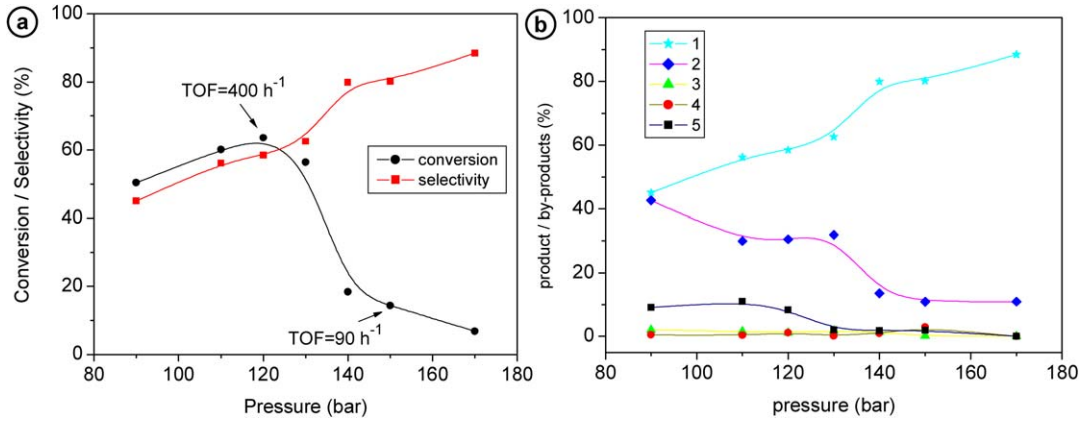

Fig. 2. Conversion of cinnamyl alcohol and selectivity to cinnamaldehyde (a), and product/byproduct distribution (b) as a function of pressure; conditions: $T = 80\,^{\circ}C$, 0.15 mol% alcohol, 0.15 mol% O_2, 1.9 mol% toluene in CO_2 (0.233 mol/min), 2.5 g of 0.5 wt% Pd/Al_2O_3.

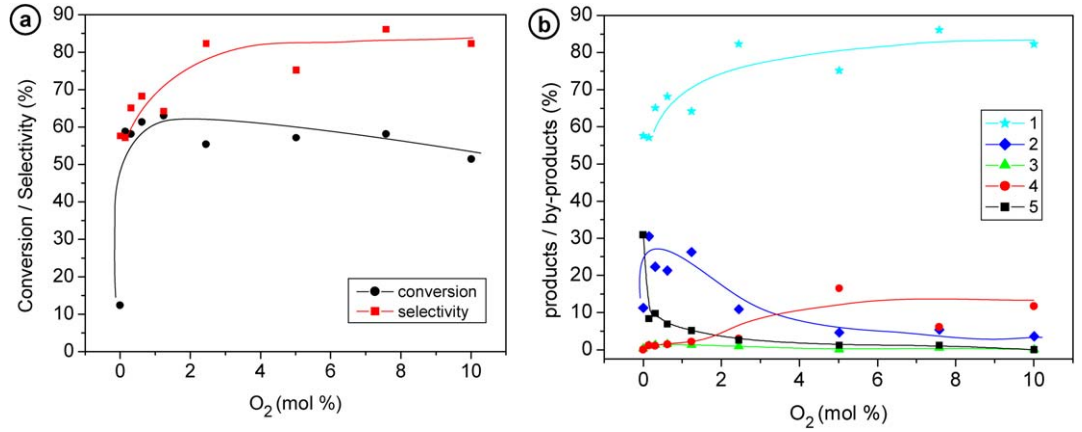

Fig. 3. Conversion of cinnamyl alcohol and selectivity to cinnamaldehyde (a), and product/byproduct distribution (b) at 120 bar as a function of oxygen concentration in the feed; conditions: 120 bar, 80 °C, 0.15 mol% alcohol, 1.9 mol% toluene in CO_2 (0.233 mol/min), 2.5 g of 0.5 wt% Pd/Al_2O_3.

transfer seemed dominant, as also indicated by the byproduct distribution. At 120 bar, the hydrogenated products 3-phenyl-1-propanol (11.2%) and beta-methylstyrene (30.9%) were detected, and at 150 bar, mainly 3-phenyl-1-propanol (19.2%) was found. Adding oxygen (0.15 mol%, same concentration of alcohol) resulted in a markedly increased reaction rate at 120 bar (Fig. 3a) with increasing alcohol conversion from 12.4 to 58.7% and a virtually unchanged selectivity to aldehyde. The byproduct distribution changed slightly, showing increased production of 3-phenyl-1-propanol (2) and decreased production of beta-methylstyrene (5). Increasing the oxygen concentration up to 10 mol% produced no clear trend, showing at first a slight increase in conversion with oxygen concentration up to 1.2%, followed by a slight deactivation. However, no strong deactivation like that observed during benzyl alcohol oxidation [22] was measured, and at 10 mol% O_2 in the feed, cinnamyl alcohol conversion was still 51.4%. The selectivity to cinnamaldehyde increased with increasing amounts of oxygen (Fig. 3). At 10 mol%, the product/byproduct distribution was 82.2% cinnamaldehyde, 11.7% benzaldehyde, and 3.6% 3-phenyl-1-propanol. Generally, with increasing oxygen partial pressure, the hydrogenated byproducts 2 and 5 decreased and the oxygenated byproduct benzaldehyde (4) increased. This striking result indicates the greater availability of surface oxygen on the palladium active sites.

In contrast, adding 0.15 mol% oxygen at 150 bar (Fig. 4) did not boost the reaction rate; compared with the oxygen-free experiment, conversion and selectivity to cinnamaldehyde remained more or less unchanged. As Fig. 4 shows, an increase in oxygen concentration resulted in an initial decrease (at 1.2 mol%), followed by a marked increase in catalytic activity. The conversion jumped from 6.4% at 1.2 mol% O_2 to 62% at 7.6 mol% O_2. A further increase to 10 mol% O_2 in the feed led to only a slight deactivation, smaller than that for benzyl alcohol [20,22]. At 10 mol%, cinnamyl alcohol conversion was 53% and selectivity to cinnamaldehyde was 72.9%. The byproduct distribution indicated the predominance of the oxygenated products, but some internal hydrogen transfer was still observed (20% of benzaldehyde vs. 5.2% of 3-phenyl-1-propanol and traces of beta-methylstyrene).

3.6. Phase behavior studies

The phase behavior of the reaction mixture was studied by video recording combined with transmission IR spectroscopy of the bulk supercritical phase and ATR-IR spectroscopy of the liquid phases. A similar approach was previously used for

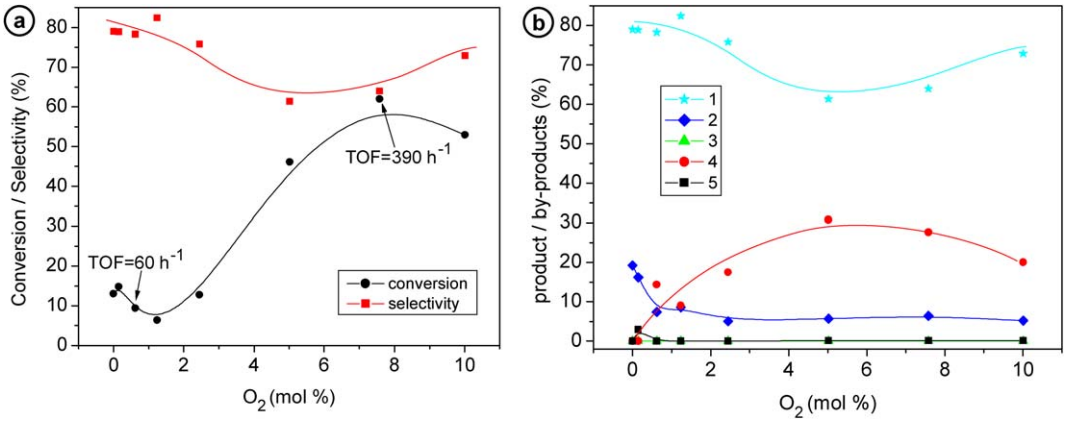

Fig. 4. Conversion of cinnamyl alcohol and selectivity to cinnamaldehyde (a), and product/byproduct distribution (b) at 150 bar as a function of oxygen concentration in the feed; conditions: 150 bar, 80 °C, 0.15 mol% alcohol, 1.9 mol% toluene in CO_2 (0.233 mol/min), 2.5 g of 0.5 wt% Pd/Al_2O_3.

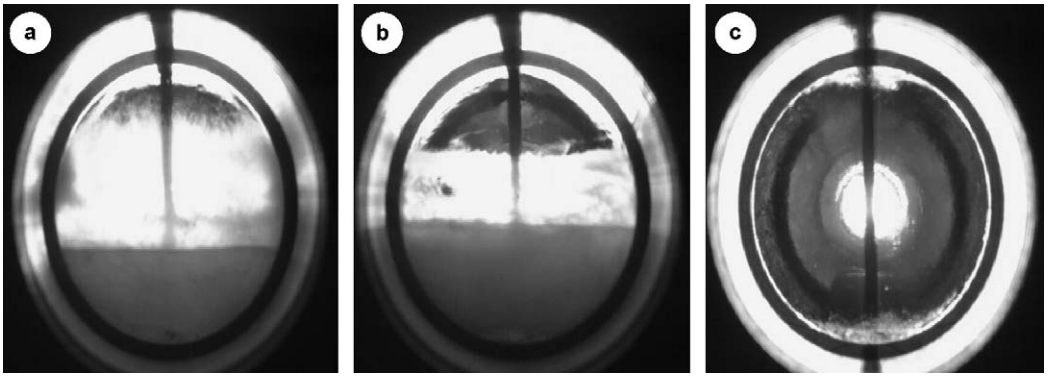

Fig. 5. Snapshots of the phase behavior of the reaction mixture in dense carbon dioxide at 80 °C and containing 0.15 mol% cinnamyl alcohol, 0.15 mol% O_2, 7.7 mol% toluene at: (a) 126.4 bar in the biphasic region; (b) 128.7 bar in the intermediate region; (c) 130.6 bar in the single phase region; (a movie of the phase transition is provided in the electronic support information).

benzyl alcohol, demonstrating that information on phase composition as well as phase behavior can be obtained [23]. Varying the amount of toluene had little effect on the transition from the biphasic region to the monophasic region of the reaction mixture. For four different compositions (1, 1.9, 7.7, and 15.4 mol% toluene in 0.15 mol% alcohol/0.15 mol% O_2/CO_2), the transition to a single supercritical phase occurred between 120 and 130 bar. Below 120 bar, at which the greatest activity was measured, all the mixtures were present as biphasic systems. This is apparent in the snapshots shown in Fig. 5, which were taken while investigating the phase behavior of the mixture containing 7.7 mol% toluene. A pressure increase of ca. 4 bar resulted in a sharp transition from a two-phase region at 126.4 bar (Fig. 5, snapshot a) via an intermediate region with a higher volume of the CO_2-expanded toluene phase at 128.7 bar (Fig. 5, snapshot b) to a single-phase region at 130.6 bar (Fig. 5, snapshot c). This phase transition can be best visualized by a movie, provided as electronic supplementary information. The phase behavior of the 1.9 mol% toluene-containing mixture (the mixture used in the parametric study) was also studied by ATR-IR spectroscopy because of the small amount of liquid present in the cell. The results are reported in Fig. 6. The transition to a single supercritical phase in the bulk started at 120 bar, as indicated by the decreased intensity of the cinnamyl alcohol bands

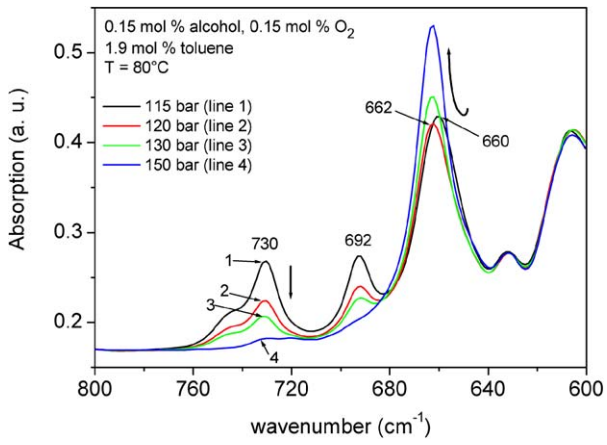

Fig. 6. ATR-IR spectra recorded at the bottom of the view cell in the ν_2-band region of CO_2 at increasing pressure for the 1.9 mol% toluene containing reaction mixture; the cinnamyl alcohol bands at 730 and 692 cm^{-1} indicate the presence of an alcohol-rich liquid-like phase at 120 bar, a transition towards a single phase is observed at high pressure by the shift of the ν_2-band of CO_2 from 660 to 662 cm^{-1} and by the decrease of the alcohol bands; (conditions: 80 °C, 0.15 mol% cinnamyl alcohol, 0.15 mol% O_2, 1.9 mol% toluene in CO_2).

at 730 and 692 cm^{-1} and the shift to higher wavenumbers of the ν_2-band of CO_2 (660 cm^{-1} at 115 bar in spectrum 1 and 662 cm^{-1} at 120 bar in spectrum 2). The shift of the ν_2-band

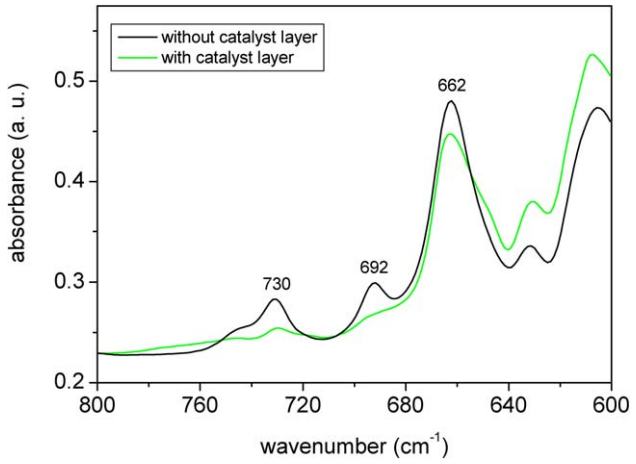

Fig. 7. Comparison of the ATR-IR spectra recorded at the bottom of the view cell of a 0.15 mol% cinnamyl alcohol, 0.15 mol% O_2, 1.9 mol% toluene in CO_2 mixture at 120 bar and 80 °C in the region of the aromatic deformation bands (730 and 692 cm^{-1}) and of the ν_2 band of CO_2 (662 cm^{-1}) recorded with and without a catalyst layer of 0.5 wt% Pd/Al_2O_3 on the ZnSe crystal; in the catalyst pores supercritical-like conditions are reached at a lower pressure (see text).

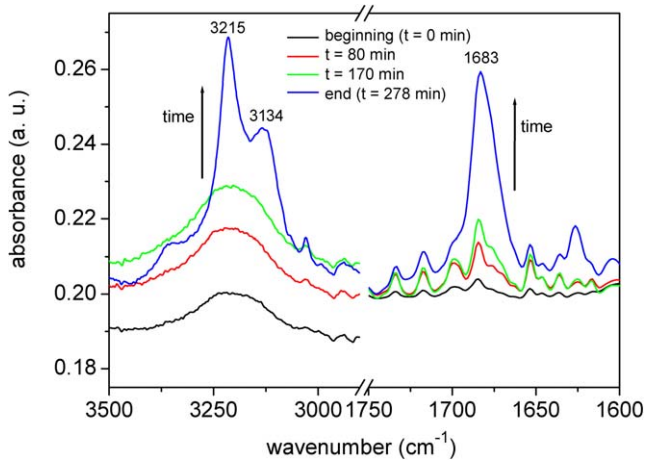

Fig. 8. On-line monitoring of the catalyst/fluid interface by ATR-IR spectroscopy during the selective oxidation of cinnamyl alcohol to cinnamaldehyde in the view cell equipped with IR spectroscopy. On the right development of the carbonyl stretching band of cinnamaldehyde (1683 cm^{-1}) during reaction, on the left rise of byproducts bands (3215 and 3134 cm^{-1}) at the end of the reaction are shown; (conditions: 120 bar, 80 °C, 0.15 mol% cinnamyl alcohol, 0.15 mol% O_2, 1.9 mol% toluene in CO_2, 5 mg of 5 wt% Pd/Al_2O_3 deposited on the crystal).

in the dense liquid-like phase is due to the interaction of CO_2 and alcohol [23,39], but alkylcarbonic acids were not found in significant amounts [40]. However, at 130 bar and after a long equilibration time, the bands of alcohol were still visible (spectrum 3), and higher pressure was needed to completely dissolve the substrate. At 150 bar, the bands of alcohol could hardly be detected (spectrum 4), as a consequence of the very short path length of the probing beam in the ATR-IR technique. However, under single-phase conditions, the ATR-IR signals reflect only the data that can also be extracted from the transmission IR results. These observations indicate a slower transformation than the sudden transformation observed for the mixture containing 7.7 mol% toluene (Fig. 5), but in this case as well, at 120 bar the mixture was still present as two phases.

3.7. Investigations at the catalyst–fluid interface by ATR-IR spectroscopy

In situ ATR-IR studies at the solid–fluid interface of the Pd-catalyst were performed by coating the ATR crystal with a layer of active catalyst with the aim of gaining information on the phase behavior inside the catalyst pores and on the interactions among CO_2, toluene, substrates, and the solid catalyst. The reaction progress was simultaneously monitored by transmission IR spectroscopy. The reaction conditions applied resembled as closely as possible those encountered during the catalytic tests in the continuous-flow reactor. In addition, experiments were performed such that the spectroscopic data and catalytic activity were reported at the same time, leading to real in situ investigations.

Interestingly, in the presence of a catalyst layer, hardly any band of cinnamyl alcohol or toluene was detected in the ATR-IR spectrum (Fig. 7) and the carbon dioxide ν_2 band was not shifted as it was in the liquid-like bulk phase. Hence the situation is similar to the single, supercritical bulk phase. This may be due to the higher virtual pressure inside narrow pores, which is known to lead to a shift in the critical temperature [41–43]; therefore, we describe the behavior inside the porous catalyst as "supercritical" even though it is well known that the critical parameters are clearly defined only in the case of pure substances [1,9,11]. In summary, the supercritical conditions observed above 150 bar in the bulk phase were reached at lower pressure and temperature in the catalyst pores.

Cinnamyl alcohol was then oxidized over the palladium catalyst at 120 bar and 80 °C in the batch reactor infrared view cell (0.15 mol% alcohol, 0.15 mol% O_2, 1.9 mol% toluene, 97.8 mol% CO_2). With increasing reaction time in the ATR-IR spectra recorded at the catalyst–fluid interface there is an increase of the cinnamaldehyde C–O stretching band at 1683 cm^{-1} (Fig. 8), whereas for the entire reaction time hardly any band of alcohol was detectable. At the end of the reaction (after ca. 280 min), the band of cinnamaldehyde was quite intense, indicating that the aldehyde was not fully dissolved in the bulk supercritical phase but remained in the catalyst pores as well. Two intense bands at 3134 and 3215 cm^{-1} also appeared, which may be assigned to byproducts containing carboxylic groups. Performing the reaction at 150 bar resulted in a lower reaction rate, in line with the observation during the catalytic tests, and during the whole reaction time bands of aldehyde or alcohol were hardly visible in the ATR-IR spectra. At the end of the reaction (after ca. 680 min), two intense bands at 3128 and 3222 cm^{-1} appeared (not shown), which were very similar to those observed at 120 bar and thus probably belong to similar types of byproducts. The conversion of cinnamyl alcohol in the batch reactor at 120 and 150 bar as a function of reaction time, calculated from the area of the cinnamaldehyde C=O stretching band is shown in Fig. 9. These measurements were taken while the phenomena were investigated at the catalyst–fluid interface and are in good accordance with the catalytic results

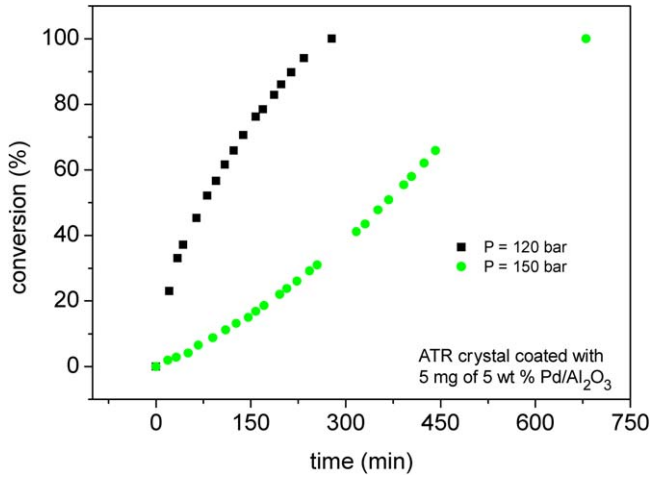

Fig. 9. Conversion as a function of time during selective oxidation of cinnamyl alcohol to cinnamaldehyde at 120 and 150 bar in the spectroscopic batch reactor view cell, extracted from the area of the carbonyl stretching band of cinnamaldehyde; conditions: $T = 80\,^{\circ}C$, 0.15 mol% cinnamyl alcohol, 0.15 mol% O_2, 1.9 mol% toluene in CO_2, 5 mg of 5 wt% Pd/Al_2O_3 deposited on the crystal.

described above. Experiments performed at 120 bar without the addition of toluene (not shown) resulted in lower catalytic activity, underlining the beneficial role of the co-solvent, which thus cannot be considered solely as a means of dissolving the solid alcohol. The phenomena at the solid–fluid interface did not differ significantly from those observed in the presence of toluene.

3.8. XAS experiments

Operando X-ray absorption experiments were performed to shed more light on the oxidation state of the palladium catalyst during cinnamyl alcohol oxidation and to investigate whether the measured changes in activity could be traced back to modifications of the catalyst structure. The X-ray absorption spectroscopic data were measured under the reaction conditions in which the catalytic activity exhibited the major changes. The experimental setup was developed to mimic as closely as possible the experiments at the synchrotron with those performed in the home laboratory [22]. Therefore, the reaction conditions applied during the XAS investigations are exactly the same (with respect to, e.g., pressure, temperature, CO_2 flow, and reactant concentration) as those typically applied in conventional experiments. The spectra, focused on the XANES region, are reported in Fig. 10a, and the corresponding Fourier-transformed EXAFS spectra are shown in Fig. 10b. The catalyst was at first reduced in 5% H_2/He at 100 °C (spectrum 1), and then exposed to a CO_2 flow (0.233 mol/min) at 120 bar and 80 °C, resulting in slight reoxidation of the palladium constituent, indicated by the decreased intensity of the Pd–Pd backscattering at 2.75 Å (Fig. 10b, spectrum 2). Cinnamyl alcohol (0.15 mol%), dissolved in toluene (1.9 mol%), was then added, with virtually no change in the EXAFS spectrum observed (not shown) but significant catalytic activity measured (Table 2). Also adding oxygen (0.15 mol%) resulted in a further slight decrease in Pd–Pd backscattering (Fig. 10b, spectrum 3). The reaction also proceeded readily in the EXAFS flow cell (Table 2); a TOF of 265 h^{-1} was measured, in line with the results of experiments in the conventional reactor (Fig. 3), emphasizing the proximity

Table 2
Catalytic activity results measured under different reaction conditions during cinnamyl alcohol oxidation over a palladium catalyst while in situ monitoring the structure of the solid catalyst by X-ray absorption spectroscopy[a]

Pressure (bar)	Alcohol (mol%)	Oxygen (mol%)	Conversion (%)	Selectivity (%)	TOF (h^{-1})	Spectrum #[b]
120	0.15	–	5.2	62.6	172	–[c]
120	0.15	0.15	8.0	45.6	265	3
120	0.15	7.0	5.7	76.6	191	–[c]
150	0.15	0.15	2.7	81.7	91	4
150	0.15	7.0	7.0	87.3	234	5
150	–	5.0	–	–	–	6

[a] Conditions: 0.4689 g of 0.5 wt% Pd/Al_2O_3 loaded in the EXAFS flow cell, $T = 80\,^{\circ}C$, 1.9 mol% toluene, 0.233 mol/min CO_2.
[b] EXAFS spectra shown in Fig. 10.
[c] Not shown.

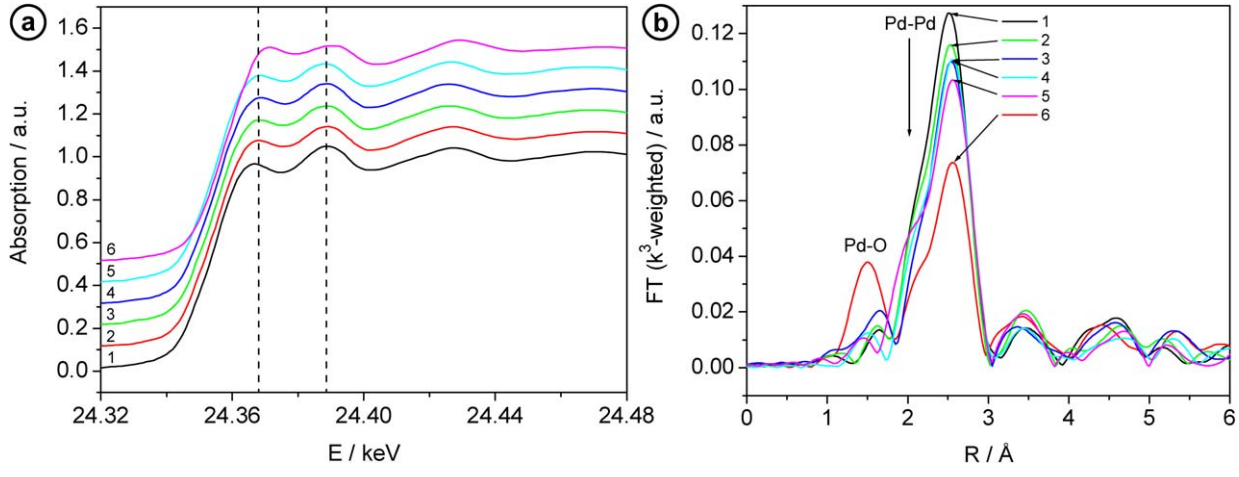

Fig. 10. In situ EXAFS investigations on a 0.5 wt% Pd/Al_2O_3 catalyst at the Pd K-edge under different reaction conditions: (a) energy-calibrated and background-corrected XANES spectra; (b) Fourier transformed EXAFS spectra; (1) in 5% H_2/He; (2) in CO_2 at 120 bar; (3) in 0.15% alcohol, 0.15% O_2, CO_2 at 120 bar; (4) in 0.15% alcohol, 0.15% O_2, CO_2 at 150 bar; (5) in 0.15% alcohol, 7% O_2, CO_2 at 150 bar; (6) in 5% O_2, CO_2 at 150 bar; (details in text).

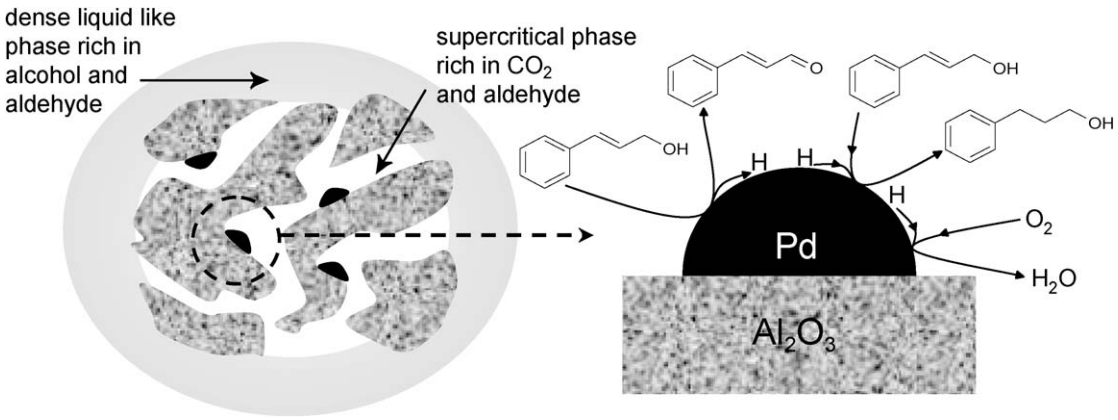

Fig. 11. Schematic representation of the phenomena taking place in the catalyst and at the Pd-particles; the presence of a dense liquid-like bulk phase, rich in aromatics, favors the dissolution of cinnamaldehyde; inside the pores mainly $scCO_2$ and cinnamaldehyde are present; the alcohol is not observed by ATR-IR spectroscopy due to a rapid dehydrogenation reaction.

to real operando studies. Increasing the oxygen concentration to 7 mol% resulted in lower catalytic activity with improved selectivity to cinnamaldehyde (Table 2), but the EXAFS spectrum remained virtually unchanged (not shown). Increasing the pressure to 150 bar (at 0.15 mol% oxygen), reaching single-phase conditions in the bulk supercritical phase, had no detectable effect on the catalyst structure, as shown by spectrum 4, which exhibited features very similar to those of spectrum 3 in both the XANES region (Fig. 10a) and the Fourier-transformed EXAFS spectra (Fig. 10b). As expected, the catalytic activity dropped, and a TOF of 91 h^{-1} was achieved under these conditions. Increasing the oxygen amount to 7 mol% at 150 bar resulted in increased activity, with the TOF rising to 234 h^{-1}, once again in agreement with the measurements performed in the conventional fixed-bed reactor (Fig. 4). Also at 7 mol% of oxygen in the feed, no significant changes were observed in the oxidation state of the palladium constituent, except for a further slight decrease in Pd–Pd backscattering (spectrum 5 in Fig. 10b). Stopping the alcohol feed, thus leaving the catalyst in 5% O_2 in CO_2 at 150 bar and 80 °C, finally resulted in oxidation of the palladium constituent. This is clearly shown by the decreased Pd–Pd feature at 24.39 keV in the near-edge region of the X-ray absorption spectrum (Fig. 10a, spectrum 6) and is also confirmed by the remarkably less intense Pd–Pd backscattering in the Fourier-transformed EXAFS spectrum (Fig. 10b, spectrum 6). Interestingly, under these conditions, Pd–O backscattering also could be clearly observed at 1.5 Å. Fitting results showed that the coordination number of Pd decreased from about 7 to 6 ($R = 2.75$ Å) and that of oxygen was about 2 ($R = 1.98$ Å).

4. Discussion

In this study, cinnamyl alcohol was oxidized by molecular oxygen for the first time in a continuous way over a palladium catalyst in supercritical carbon dioxide. The reaction rate was significantly higher than that in conventional organic solvents [16,44]. A strong dependence of reaction rate on pressure and oxygen concentration was found (Figs. 2–4), with high performance achieved in the low-pressure region (90–120 bar) and at high oxygen concentration (5–8 mol%). However, the selectivity pattern and spectroscopic investigations indicated different reaction pathways in these two regions of high catalytic performance than those observed in liquid-phase oxidation [45].

The effect of pressure on reaction rate can be traced back to the characteristic phase behavior of the reaction mixture (Fig. 5). At low pressure, two phases were present in the bulk, with a CO_2-rich gas-like phase (containing also part of the cinnamyl alcohol and almost all of the toluene) in equilibrium with an alcohol-rich liquid-like phase (Figs. 5 and 6). The higher activity in the biphasic region of the bulk-phase behavior is opposite to that reported for benzyl alcohol [20,23] and clearly indicates that the transition to a single bulk phase has a negative influence on the reaction rate. Hence, gas–liquid mass transfer is not rate-limiting. Whereas the bulk phase is present at 120 bar as a biphasic reaction mixture with a dense liquid-like phase probably in contact with the catalyst particles (as suggested by the ATR-IR investigations performed without coating the catalyst on the crystal), ATR-IR spectroscopy, performed by coating the crystal with a layer of an active catalyst, suggests that the conditions inside the pores resemble the situation found in the bulk phase under single-phase conditions (e.g., rich in carbon dioxide). This situation is shown schematically in Fig. 11. A liquid-like phase in the bulk is probably beneficial because it leads to a higher alcohol concentration around the particles and exhibits a higher solvation power, which is beneficial for the extraction (i.e., desorption and transport) of the aldehyde and the byproducts, including water. Cinnamaldehyde was observed inside the porous catalyst (cf. Fig. 8), whereas this was not the case for benzaldehyde, which can also be well dissolved by supercritical carbon dioxide [23,46].

The selectivity pattern under these conditions indicates a high hydrogen concentration on the catalyst surface. In fact, alcohol oxidation over noble metal catalyst proceeds via oxidative dehydrogenation, the first step being the adsorption and dehydrogenation of the alcohol to the corresponding aldehyde or ketone [16,47]. The hydrogen thus formed can be removed either by oxidation with molecular oxygen [45] or, in the case of cinnamyl alcohol, by internal hydrogen transfer [48], as indicated in Fig. 11. The high catalytic activity at oxygen-free conditions and 3-phenyl-1-propanol (2) as the main byproduct both

in the presence and in the absence of oxygen reveals that the reaction readily proceeds by internal hydrogen transfer and that hydrogen is available on the catalyst surface in high concentration. This also favors hydrogenolysis reactions, as indicated by the high concentration of beta-methylstyrene (5) in the effluent. Interestingly, despite the high concentration of surface hydrogen, propylbenzene (from the hydrogenation of the C=C double bond of beta-methylstyrene) was detected only in traces. Higher amounts of beta-methylstyrene than in liquid phase oxidation were found [24,45] and this difference can probably be traced back to its higher affinity for $scCO_2$. As soon as it is formed, it quickly desorbs and diffuses out of the catalyst pores without further reaction.

The increased reaction rate at 150 bar and high oxygen concentration (5–8 mol%; Fig. 4) may be attributed to a change in bulk-phase behavior, because the reaction mixture becomes biphasic at high O_2 concentrations, as expected based on the decrease in overall density [49]. But the phase composition/behavior inside the catalyst pores remained unchanged. Again, two phases in the bulk phase and supercritical-like conditions inside the catalyst pores led to a high catalytic activity. The reaction pathway at high oxygen concentration is different, as indicated by the byproduct distribution, which showed benzaldehyde as the main byproduct. Benzaldehyde can be formed from cinnamic acid by oxidative cleavage of the carbon–carbon double bond. This reaction is discussed in the literature, even though it requires severe reaction conditions with strong oxidants [50–52]. In the present case, the reaction may be favored by rapid removal of benzaldehyde due to its high solubility in supercritical carbon dioxide [23,46,53], which continuously shifts the equilibrium of the reaction toward benzaldehyde. Cinnamic acid was observed in only trace amounts during the catalytic tests, whereas carboxylic species at the catalyst–fluid interface were detected by infrared spectroscopy (Fig. 8). It may be formed by acid-catalyzed hydration with the co-product water of cinnamaldehyde, followed by oxidative dehydrogenation of the hydrate [54]. Interestingly, in the experiment performed at 120 bar, benzaldehyde was the main byproduct only above 5 mol% of oxygen in the feed, whereas at 150 bar it was the main byproduct already at ca. 1 mol% of oxygen. This again may be traced back to the bulk-phase behavior. At 150 bar, supercritical conditions in the bulk imply improved external mass transfer and thus higher oxygen concentration at the catalyst surface. From previous results [31], we can exclude the possibility that benzaldehyde is derived from the oxidation of toluene. Typically, the reaction occurs at higher temperatures [55,56].

Oxygen has thus a strong influence on the phase behavior and on the reaction pathway, but in contrast to the previous observation with benzyl alcohol [20,22] it did not play a direct role in catalyst deactivation. Up to 10 mol% of oxygen in the feed no strong deactivation could be observed (Figs. 3 and 4). In principle, deactivation due to over-oxidation may take place when the oxygen supply on the catalyst is higher than its consumption by the reactions, thus leading to a surface oxidation of the palladium constituent [14,16,24,57,58]. In the present case no deactivation due to over-oxidation of the catalyst surface was observed due to the high concentration of surface hydrogen available under all the reaction conditions investigated. In situ XAS studies support this conclusion. Under almost all the experimental conditions investigated the palladium constituent was found to be in an almost fully reduced state during alcohol oxidation. Because an increase in pressure from 120 to 150 bar (at 0.15 mol% of oxygen in the feed) resulted in no changes in the catalyst structure, we can exclude the possibility that the liquid-like phase present in the bulk protected the catalyst from overoxidation, by, for instance, decreasing the diffusion rate of oxygen. In addition, also at high oxygen concentration (7 mol%), no significant oxidation of the palladium constituent was observed (Fig. 10). Interestingly, only when the alcohol feed was stopped, thus leaving the catalyst in 5 mol% O_2/CO_2, did an evident oxidation of the surface palladium occur. This underscores the role of surface hydrogen in preventing oxidation of the catalyst and indicates that the dehydrogenation step actually proceeds. The results are also in good agreement with the observed byproduct distribution, particularly of the products of hydrogenolysis. The internal hydrogen transfer is a very sensitive probe for Pd–H species on the surface. Also at high oxygen concentration, even though benzaldehyde was the major byproduct, 3-phenyl-1-propanol (2) and 3-phenyl propionaldehyde (3), derived from internal hydrogen transfer (Scheme 2), were still present in considerable amounts, demonstrating that even under these conditions hydrogen is still available on the palladium surface.

5. Conclusion

In this paper we have presented a simple and effective method for the continuous selective oxidation of solid cinnamyl alcohol in supercritical carbon dioxide over a heterogeneous palladium catalyst. Using toluene as a co-solvent allowed the reaction to be performed efficiently and in a continuous manner. During optimization, a high reaction rate with a TOF of 400 h^{-1} and selectivity to cinnamaldehyde of ca. 60% was achieved. A marked dependence on pressure and oxygen concentration was found. Depending on the different reaction conditions, hydrogenation, hydrogenolysis, and oxidative cleavage of carbon–carbon double bonds were observed as side reactions. Phase behavior studies, in situ transmission and ATR-IR spectroscopy, as well as operando XANES/EXAFS studies, were excellent tools for gaining deeper insight into the reaction mechanism, the solid/fluid interface, and the state of the catalyst. The oxidation reaction is significantly different to benzyl alcohol oxidation in supercritical carbon dioxide. In contrast to benzyl alcohol oxidation, a biphasic reaction mixture was beneficial for the catalytic performance of the Pd-catalyzed oxidation of cinnamyl alcohol, and no deactivation due to oxygen in high concentration was observed. Both the reaction network and the in situ XANES and EXAFS studies under reaction conditions revealed that Pd was mainly in the metallic state, even in the presence of high amounts of oxygen. In addition, IR-spectroscopic studies at the solid–fluid interface indicated that the phase composition was significantly different in the catalyst pores than in the bulk phase, particularly under reaction condi-

tions. This indicates that a good understanding of the fluid or reaction mixture inside a porous catalyst is inevitable at near- or supercritical conditions.

Acknowledgments

The authors gratefully acknowledge the Swiss Federal Office of Energy (BFE) for financial support and Engelhard Italiana S.r.l. for providing the catalyst samples. They also thank the Hamburger Synchrotron Labor (HASYLAB) at DESY (Hamburg, Germany) for beam time and Dr. E. Welter for the support during the measurements. This work at the synchrotron radiation source was supported by the European Community - Research Infrastructure Action under the FP6 Structuring the European Research Area program (through the Integrated Infrastructure Initiative [Integrating Activity on Synchrotron and Free Electron Laser Science] contract RII3-CT-2004-506008). Thanks are due to Drs. T. Mallat, D. Ferri, and C. Keresszegi for help and discussion, and to R. Mäder and P. Trüssel (mechanical workshop, ETH Zürich) for their continuous technical assistance. Dr. M. Burgener is acknowledged for the help during the phase-behavior measurements, and SITEC Sieber Engineering AG is recognized for their steady interest and continuous support.

Electronic support information available

A movie recorded while investigating the phase behavior of a 0.15 mol% alcohol/0.15 mol% O_2/7.7 mol% toluene in CO_2 is available from the web pages of *Journal of Catalysis*.

Please visit DOI:10.1016/j.jcat.2006.03.009.

References

[1] P.G. Jessop, W. Leitner, Chemical Synthesis Using Supercritical Fluids, Wiley–VCH, Weinheim, 1999.
[2] A. Baiker, Chem. Rev. 99 (1999) 453.
[3] P.G. Jessop, T. Ikariya, R. Noyori, Chem. Rev. 99 (1999) 475.
[4] A.D. Kasnevich, E.J. Beckman, Chem. Today June 2004 (2004) 38.
[5] E.J. Beckman, J. Supercrit. Fluids 28 (2004) 121.
[6] G. Musie, M. Wei, B. Subramaniam, D.H. Busch, Coord. Chem. Rev. 219 (2001) 789.
[7] J.R. Hyde, P. Licence, D. Carter, M. Poliakoff, Appl. Catal. A 222 (2001) 119.
[8] H. Jin, B. Subramaniam, Chem. Eng. Sci. 58 (2003) 1897.
[9] J.-D. Grunwaldt, R. Wandeler, A. Baiker, Catal. Rev.-Sci. Eng. 45 (2003) 1.
[10] S. Campestrini, U. Tonnellato, Curr. Org. Chem. 9 (2005) 31.
[11] R. Wandeler, A. Baiker, CATTECH 4 (2000) 128.
[12] J.-D. Grunwaldt, A. Baiker, Phys. Chem. Chem. Phys. 7 (2005) 3526.
[13] M. Besson, P. Gallezot, Catal. Today 57 (2000) 127.
[14] J.H.J. Kluytmans, A.P. Markusse, B.F.M. Kuster, G.B. Marin, J.C. Schouten, Catal. Today 57 (2000) 143.
[15] J. Muzart, Tetrahedron 59 (2003) 5789.
[16] T. Mallat, A. Baiker, Chem. Rev. 104 (2004) 3037.
[17] G. Jenzer, M.S. Schneider, R. Wandeler, T. Mallat, A. Baiker, J. Catal. 199 (2001) 141.
[18] A.M. Steele, J. Zhu, S.C. Tsang, Catal. Lett. 73 (2001) 9.
[19] R. Gläser, R. Jos, J. Williardt, Top. Catal. 22 (2003) 31.
[20] M. Caravati, J.-D. Grunwaldt, A. Baiker, Catal. Today 91–92 (2004) 1.
[21] S.C. Tsang, J. Zhu, A.M. Steele, P. Meric, J. Catal. 226 (2004) 435.
[22] J.-D. Grunwaldt, M. Caravati, M. Ramin, A. Baiker, Catal. Lett. 90 (2003) 221.
[23] M. Caravati, J.-D. Grunwaldt, A. Baiker, Phys. Chem. Chem. Phys. 7 (2005) 278.
[24] J.-D. Grunwaldt, C. Keresszegi, T. Mallat, A. Baiker, J. Catal. 213 (2003) 291.
[25] A.F. Lee, K. Wilson, Green Chem. 6 (2004) 37.
[26] C. Keresszegi, T. Mallat, J.-D. Grunwaldt, A. Baiker, J. Catal. 225 (2004) 138.
[27] M.S. Schneider, J.-D. Grunwaldt, T. Bürgi, A. Baiker, Rev. Sci. Instrum. 74 (2003) 4121.
[28] T. Ressler, J. Synchr. Rad. 5 (1998) 118.
[29] Z. Hou, B. Han, L. Gao, Z. Liu, G. Yang, Green Chem. 4 (2002) 426.
[30] Y. Chang, T. Jiang, B. Han, L. Gao, R. Zhang, Z. Liu, W. Wu, Ind. Eng. Chem. Res. 42 (2003) 6384.
[31] M. Caravati, J.-D. Grunwaldt, A. Baiker, Appl. Catal. A 298 (2006) 50.
[32] M. Wei, G.T. Musie, D.H. Busch, B. Subramaniam, J. Am. Chem. Soc. 124 (2002) 2513.
[33] B. Kerler, R.E. Robinson, A.S. Borovik, B. Subramaniam, Appl. Catal. B 49 (2004) 91.
[34] J.M. Dobbs, J.M. Wong, K.P. Johnston, J. Chem. Eng. Data 31 (1986) 303.
[35] J.M. Dobbs, J.M. Wong, R.J. Lahiere, K.P. Johnston, Ind. Eng. Chem. Res. 26 (1987) 56.
[36] C.A. Eckert, K. Chandler, J. Supercrit. Fluids 13 (1998) 187.
[37] C.A. Eckert, D. Bush, J.S. Brown, C.L. Liotta, Ind. Eng. Chem. Res. 39 (2000) 4615.
[38] D.M. Ginosar, B. Subramaniam, J. Catal. 152 (1995) 31.
[39] S.G. Kazarian, M.F. Vincent, F.V. Bright, C.L. Liotta, C.A. Eckert, J. Am. Chem. Soc. 118 (1996) 1729.
[40] K.N. West, C. Wheeler, J.P. McCarney, K.N. Griffith, D. Bush, C.L. Liotta, C.A. Eckert, J. Phys. Chem. A 105 (2001) 3947.
[41] L.D. Gelb, K.E. Gubbins, R. Radhakrishnan, M. Sliwinska-Bartkowiak, Rep. Prog. Phys. 62 (1999) 1573.
[42] K. Morishige, M. Ito, J. Chem. Phys. 117 (2002) 8036.
[43] M.S. Schneider, J.-D. Grunwaldt, A. Baiker, Langmuir 20 (2004) 2890.
[44] T. Mallat, Z. Bodnar, P. Hug, A. Baiker, J. Catal. 153 (1995) 131.
[45] C. Keresszegi, T. Bürgi, T. Mallat, A. Baiker, J. Catal. 211 (2002) 244.
[46] D. Walther, G. Maurer, Ber. Bunsen.-Ges. Phys. Chem. 96 (1992) 981.
[47] C. Keresszegi, D. Ferri, T. Mallat, A. Baiker, J. Catal. 234 (2005) 64.
[48] C. Keresszegi, T. Mallat, A. Baiker, New J. Chem. 25 (2001) 1163.
[49] J. Chrastill, J. Phys. Chem. 86 (1982) 3016.
[50] I.G. Aguilar, P.R. Rey, C. Baluja, Ozone Sci. Eng. 23 (2001) 177.
[51] D.G. Lee, T. Chen, Z. Wang, J. Org. Chem. 58 (1993) 2918.
[52] S. Lai, D.G. Lee, Synthesis 11 (2001) 1645.
[53] D. Walther, G. Maurer, J. Chem. Eng. Data 38 (1993) 247.
[54] P. Vinke, H.E. van Dam, H. van Bekkum, Stud. Surf. Sci. Catal. 55 (1990) 147.
[55] C.-C. Guo, Q. Liu, X.-T. Wang, H.-Y. Hu, Appl. Catal. A 282 (2005) 55.
[56] K.M. Dooley, F.C. Knopf, Ind. Eng. Chem. Res. 26 (1987) 1910.
[57] C. Keresszegi, J.-D. Grunwaldt, T. Mallat, A. Baiker, J. Catal. 222 (2004) 268.
[58] H.E. van Dam, A.P.G. Kieboom, H. van Bekkum, Appl. Catal. 33 (1987) 361.